Hindawi
Advances in Civil Engineering
Volume 2021, Article ID 4321255, 12 pages
https://doi.org/10.1155/2021/4321255

Research Article

Accurate Perception of Rock Strata Movement for Environmental Protection in Coal Mining: Taking Thick and Hard Roof Cooperative Control as an Example

Tong Zhao,[1] **Changyou Liu**,[2] **Kaan Yetilmezsoy**,[3] **Majid Bahramian**,[4] **and Peilin Gong**[5]

[1]*Key Laboratory of In Situ Modified Mining Ministry of Education, Taiyuan University of Technology, Taiyuan, Shanxi 30024, China*
[2]*State Key Laboratory of Coal Resources and Safe Mining, School of Mines, China University of Mining & Technology, Xuzhou 221116, China*
[3]*Department of Environmental Engineering, Faculty of Civil Engineering, Yildiz Technical University, Davutpasa Campus, Esenler, Istanbul, 34220, Turkey*
[4]*School of Chemical and Bioprocess Engineering, University College Dublin, Belfield, Dublin, Ireland*
[5]*College of Mining Technology, Taiyuan University of Technology, Taiyuan, Shanxi 30024, China*

Correspondence should be addressed to Changyou Liu; tb14020023@cumt.edu.cn

Received 21 June 2021; Accepted 11 October 2021; Published 1 November 2021

Academic Editor: Yingchun Li

Accurate perception of the key stratum instability can improve the safety of coal mining and also provide a basis for alleviating overlying rock strata destruction and environmental disturbance. To efficiently evaluate the instability of the key stratum and its threat to safe mining and environmental protection, the fracture characteristics and weakening mechanisms were studied through physical simulation, theoretical analysis, and field measurement. A scheme and the parameters of confined blasting in water-filled deep hole presplit technology (CBWDHPT) for thick and hard roof (THR) weakening were proposed. Research studies showed that, after the THR fractured into large blocks, the subsequent sliding instability induced serious support-crushing accidents; however, increasing the support strength could only provide limited control. Confined water and infiltrated modified rock mass functioned as the transfer load medium of the explosives, and the CBWDHPT fully utilized high explosion energy to break rocks. Consequently, the collapse and filling of the immediate roof and low-positioned THR, as well as the timely cutting off the middle-positioned THR, could be realized, which alleviated the migration space of THR blocks, overlying strata destruction, and earth-surface step subsidence. Finally, the environmentally friendly strategy (including the CBWDHPT and hydraulic support optimization) for overlying rock strata protection was proposed. In the industrial test, the THR was broken into blocks of different sizes after utilizing the CBWDHPT, and the support working resistance was significantly decreased. It was concluded that the environmentally friendly strategy could effectively reduce the risk of overlying rock strata destruction.

1. Introduction

Safety, efficiency, and environmentally friendly are the goals of coal mining. A series of mining-induced environmental and ecological damages such as groundwater level drop [1, 2], surface subsidence [3], and ecological destruction put forward high requests for the key stratum control. Different strata react distinctly to the mining, and the accurate perception of the fracture, migration, and instability laws of the key stratum was the prerequisite for alleviating the destruction of the overlying rock strata. With high strength, large layer thickness, and good integrity, thick and hard roof (THR), mainly consisting of sandstone and conglomerate, served as the key stratum and formed large overhangs during mining [4]. A strong and hard hanging roof caused high underground stress in underground mines, leading to

rockburst, coal and gas outburst, and earth-surface step subsidence. Coal seams with THR account for approximately one-third of the total in China, and they are distributed in more than 50% of coalfields, such as Datong and Jincheng [5]. THR, especially those in direct contact with coal seams, had a significantly different mining response from that of high-positioned THR, which made their control and safe mining extremely difficult [6, 7]. These problems could not be solved by simply increasing the support intensity, creating new challenges for roof control.

The main approach to THR control was to modify the physical and mechanical properties of the roof and decrease the collapse thickness and tensile strength of the rock mass, thereby proposing the roof weakening and softening perception. At present, deep-hole blasting and hydraulic fracturing were mainly used for coal rock weakening [8]. Deep-hole blasting caused a low explosion energy utilization rate, massive amounts of dust and harmful gas, and a poor control effect [9, 10]. Meanwhile, the high-pressure (60 MPa) water equipment used in hydraulic fracturing had difficulty in meeting the safety requirements of THR control [11, 12].

Aiming at the safe mining of thick and hard main roofs with a thin or even without immediate roof, physical simulation, theoretical analysis, and field measurement were adopted. The research was structured as follows: structural characteristics and instability migration rules of THR, which directly contacted the coal seam, are presented in Section 1. The mechanical model and working resistance calculation of THR in the initial fracture are analyzed in Section 2. Precontrol technology for THR is explored in Section 3: (1) weakening mechanism of THR with the confined blasting in water-filled deep hole presplit technology (CBWDHPT); (2) computational analysis of the weakening effect of the CBWDHPT. Lastly, a useful collaborative control technology, which combined the confined blasting in water-filled deep hole presplit and hydraulic support optimization, is put forward to provide a reference for environmental protection in coal mining.

2. Materials and Methods

2.1. Engineering Geological Conditions. Distributed in the north-wing mining area of Zhuxianzhuang Coal Mine, a conglomerate layer acted as the key stratum, which had a dip angle of 15°–25°, an average thickness of 60 (±5) m, and a compressive strength of 67.79 MPa. On working face 880 with the wedge-structure immediate roof, the mined 9.60 m-thick 8# coal was at a close distance with the THR. As shown in Figure 1, the working face length was 165 m, the walking length was 400 m, and the long wall fully mechanized top coal caving technology was adopted.

It was known from the key strata theory that the conglomerate had great thickness, high strength, and good integrity, which served as the main roof. The immediate roof under the conglomerate was composed of mudstone and sandy mudstone with low strength and small thickness. It collapsed with the working face advancing and filled the goaf.

2.2. Structural Characteristics and Instability Migration Rules of the THR at a Close Distance. In this study, considering the geological conditions, a physical simulation model of thick coal seam is established, and the THR fracture characteristics and instability migration rules are further analyzed.

Based on previous studies, small immediate roof thickness, weak supporting intensity, and large THR caving space resulted in a strong impact on the working face [13]. The support load reached the critical value and created a highly dangerous working condition, with THR directly contacting the coal seam and the immediate roof lacking, which was selected as the engineering background of the study.

2.3. Model Construction and Parameter Setting. According to the working face 880 conditions, the model parameters were determined as follows: (i) geometric similarity ratio was 1 : 120, (ii) gravimetric ratio was 1 : 1.56, (iii) stress similarity ratio was 1 : 187.2, (iv) dynamic load similarity ratio was 1 : 2695680, (v) time similarity ratio was 1 : 10.95, and (vi) speed similarity ratio was 1 : 1314.53. The model was developed on a plane stress platform (2.5 m long × 2.0 m high × 0.2 m wide) as shown in Figure 2, in which there were three horizontal measuring lines, 10 vertical measuring lines, and 29 vertical stress monitoring points. The physical-mechanical parameters are listed in Table 1.

The simulation had two steps: step one was the preparation stage: designing the model and establishing the loading system and monitoring system; additionally, the self-weight of the 250 m rock strata was loaded with air pump pressure 0.02929 MPa. Step two was the mining stage: setting boundary pillars (300 mm wide, actual width was 36 m) at both ends of the model and mining with cutting height 80 mm and excavation footage 50 mm [13, 14].

3. Results and Discussion

3.1. Structural Characteristics of the THR during the First Weighting Stage. With the excavation of the coal seam, the THR continued to become exposed. When the working face advanced to 120 m from the setup entry, because of great self-strength, a large area of the THR overhung without collapsing. The exposed THR bent down and sank continuously, and a vertical tension crack (18 m long) appeared on the lower surface of the THR (nearly the midpoint of the span). Because the strata were extremely thick, the fracture was not well versed throughout the rock; however, the bottom of the THR experienced tension failure, as shown in Figure 3.

When the working face moved to 138 m away from the setup entry, the hanging THR suddenly broke and collapsed, and the first weighting occurred. Directly contacting the coal seam, the conglomerate had no collapsed gangue to support it; therefore, a large free migration space was created before its collapse. The fractured THR violently slid and sank into the goaf, and the vertical crack on the lower surface of the strata penetrated all the strata. Because of large thickness, high density and hardness, and good integrity, a huge block

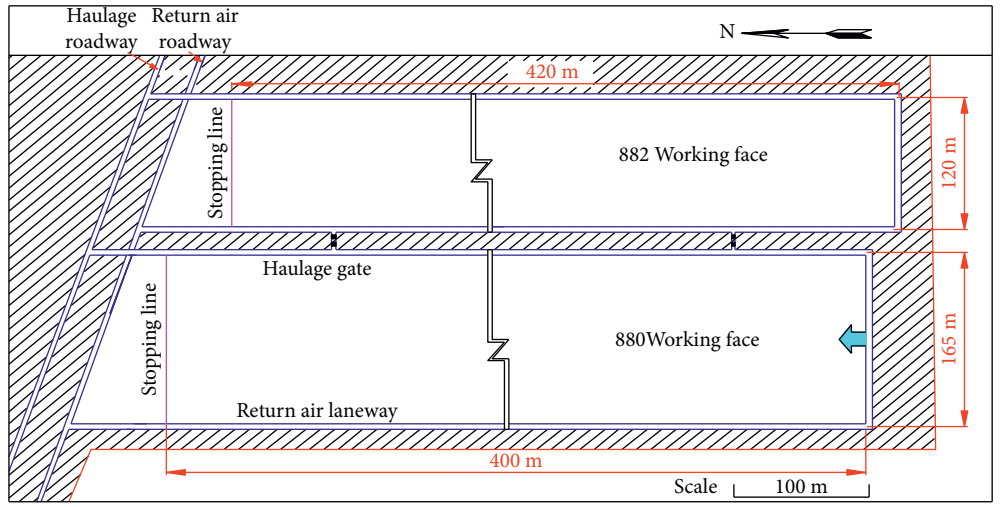

Figure 1: Layout of working face 880 under the THR.

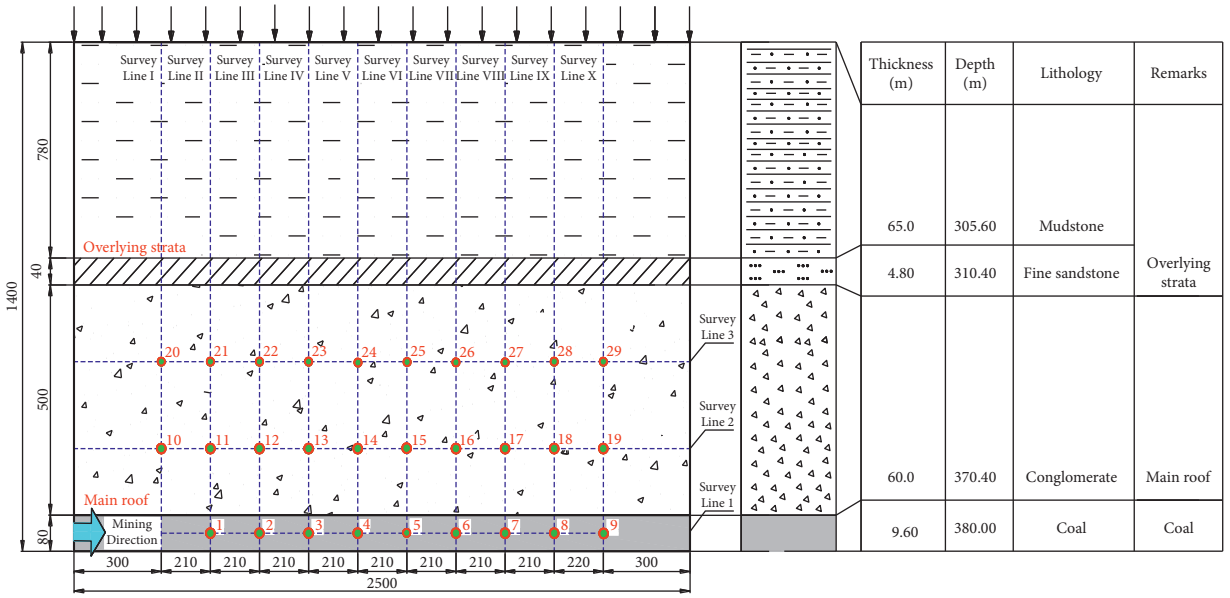

Figure 2: Stope model of extra-thick coal seam mining under the THR.

Table 1: Physical-mechanical parameters and ratio of coal rock in the model.

Name	Thickness (m)	Tensile strength (MPa)	Modulus of elasticity (GPa)	Cohesion (MPa)	Compressive strength (MPa)		Volume weight (g/cm^3)		Matching
					Prototype	Model	Prototype	Model	Sand : plaster : lime
Sandy mudstone	65.0	6.45	5.72	2.17	42.47	0.23	2.65	1.70	4 : 3 : 7
Fine sandstone	4.80	9.57	3.72	1.98	69.58	0.37	2.64	1.69	4 : 3 : 7
Conglomerate	60.0	4.50	1.79	7.30	67.79	0.36	2.72	1.74	3 : 3 : 7
Mudstone	1.20	2.61	0.99	3.87	19.01	0.10	2.51	1.61	3 : 7 : 3
Fine sandstone	4.20	11.56	2.72	9.15	69.76	0.37	2.64	1.69	4 : 3 : 7
Mudstone	6.36	3.06	3.06	1.94	7.42	0.0.4	2.34	1.50	3 : 7 : 3
8# coal	9.60	1.05	1.98	1.63	7.78	0.15	1.43	0.91	5 : 3 : 7

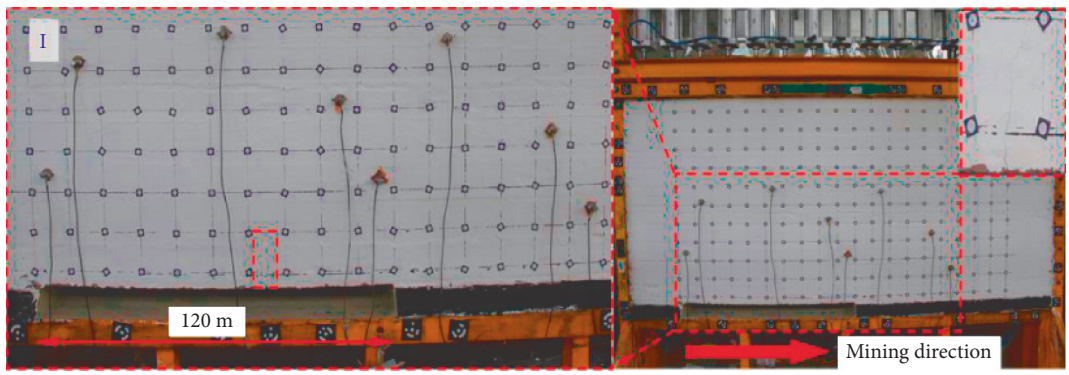

(a)

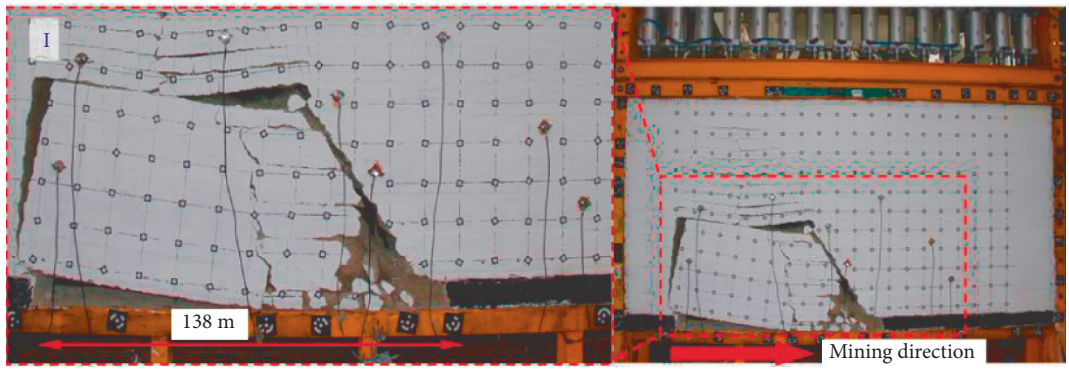

(b)

Figure 3: Instability migration rules of overlying strata in mining. (a) The working face advanced to 120 m. (b) The working face advanced to 138 m.

structure was formed after the initial fracture of the THR, as depicted in Figure 3(b).

Because of the large area and long hanging time before the initial fracture, the roof deformation and potential energy reached the limit value in an extremely unstable state, which developed into a fractured condition when the working face continued advancing. The high mining height and support absence from collapsed gangue in the goaf caused the THR blocks to sink violently. The potential energy accumulated in the roof was converted into kinetic energy, and a large amount of energy was released simultaneously.

3.2. Mechanical Model and Working Resistance Calculation during the First Weighting Stage. During the first weighting stage, the THR broke into a huge block (block AB) under the self-weight and the overlying load (Figure 4). To stabilize the block, the supporting intensity should balance the instability load of block AB and prevent overall instability and hydraulic support crushing [15]. The mechanical model of block AB was established, as shown in Figure 5.

In Figure 5, T is the horizontal binding (kN), G is the self-weight of the THR block (kN), F is the friction force on the block (kN), θ is the angle between the main roof fracture line and the vertical line (°), ϕ is the basic friction angle of the block (°), β is the fracture angle of the THR (°), q_0 is the equivalent uniform live load of the self-weight of soft strata (kN/m), L_0 is the first weighting distance of the THR (m), H is the thickness of the THR (m), and m is the thickness of the coal seam (m).

According to Figure 5, to prevent block AB from being unstable, friction force F, self-weight V, and the load of the overlying strata needed to meet the following condition [15]:

$$F = T\tan(\theta \pm \phi) \geq V. \tag{1}$$

Analyzing the mechanical model, the moment equilibrium of point O and the force equilibrium conditions in the vertical direction were obtained as follows (Wu et al., 2019):

$$\begin{cases} \sum M_O = 0, \\ \sum F_{Oy} = 0, \end{cases} \tag{2}$$

$$\begin{cases} V = \dfrac{L_0 b\gamma H + \gamma_3 H_3}{2}, \\ T = \dfrac{{L_0}^2 b\gamma H + \gamma_3 H_3}{8H(1 - Kg)}, \end{cases} \tag{3}$$

where L_0 is the length of the fractured block AB, which is approximately equal to the first weighting distance of the conglomerate (m), b is the width of a single hydraulic support (m), γ and γ_3 are the bulk densities of the conglomerate and the overlying soft strata, respectively (kN/m^3), H and H_3 are the thicknesses of the conglomerate and

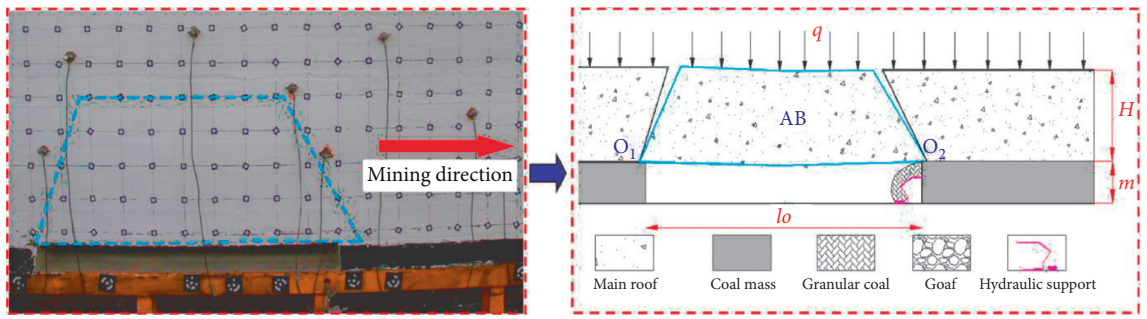

Figure 4: Fracture structure model of the THR first weighting at a close distance.

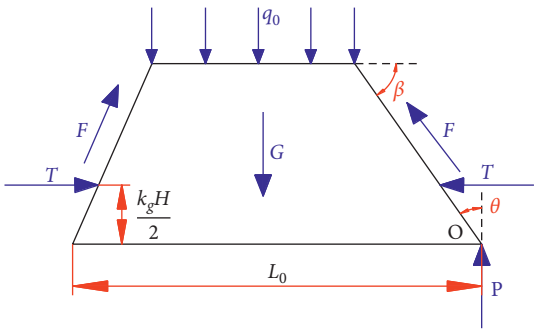

Figure 5: Fractured block force analysis of the THR first weighting at a close distance.

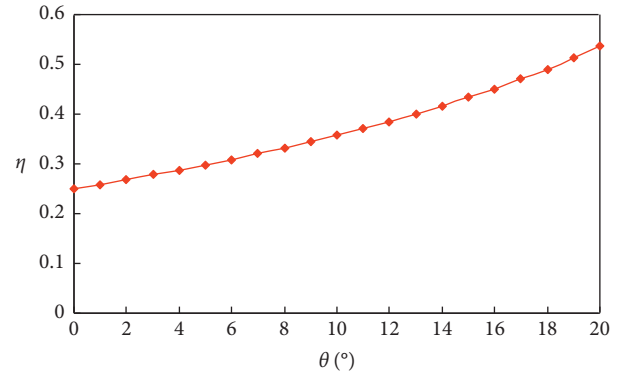

Figure 6: Relationship between θ (angle between the fracture line and vertical line) and η (ratio of thickness to span) during the first weighting.

the overlying soft strata, respectively (m), and Kg is the extrusion height coefficient of the hinged structure, $Kg = 0.018H - 0.0195$.

Substituting V and T into equation (1), the equilibrium condition was obtained as follows [16]:

$$\frac{H}{L_0} \le \frac{1}{4}\tan(\theta \pm \phi). \tag{4}$$

The thickness-to-span ratio of the fractured block is $\eta = H/L_0$, and the friction angle of the block is $\phi = 38^\circ$–45°. The friction force between the fractured block AB and the working face-side rock must satisfy $F = T(1/4)\tan(\theta + \phi)$, and the condition without block AB sliding instability was obtained as follows:

$$\eta \le \frac{1}{4}\tan(\theta + \phi). \tag{5}$$

The relationship between θ (the angle between the fracture line and vertical line) and η (the ratio of thickness to span) was obtained through fitting, as shown in Figure 6.

To balance the sliding load of block AB, the effective support force P and vertical friction force F along the fracture line must be no less than the vertical load V and the top coal self-weight Q within the roof control distance [17].

$$P = V + Q - F, \tag{6}$$

$$F = T \cdot f, \tag{7}$$

$$\begin{cases} Q = \gamma_1 m_2 \cdot ab, \\ f = \tan\left(J_{RC}\lg\dfrac{KgHJ_{CS}}{T} + \varphi_b + \beta - \dfrac{\pi}{2}\right), \end{cases} \tag{8}$$

where a is the effective roof control distance (m), m_2 is the caving thickness (m), β is the fractured angle of the THR block (°), φ_b is the basic friction angle (°), γ_1 is the bulk density of the top coal (kN/m^3), f is the friction coefficient, J_{RC} is the roughness coefficient of the fractured surface of the conglomerate, J_{CS} is the effective compressive strength of the fractured surface of the conglomerate considering the compressive strength (MPa), and q_0 is the self-weight of the overlying strata, $q_0 = \gamma_3 H_3$ (MPa).

Substituting equations (7) and (8) into (6) yielded the following equation:

$$P = V - T\tan\left(J_{RC}\lg\frac{KgHJ_{CS}}{T} + \varphi_b + \beta - \frac{\pi}{2}\right) + \gamma_1 m_2 \cdot ab. \tag{9}$$

Substitute equations (2) and (3) into (9), which can be simplified to the equation as follows:

$$P = \frac{L_0 q}{2} - \frac{{L_0}^2 q}{8H(1 - Kg)}\tan\left(J_{RC}\lg\frac{KgHJ_{CS}}{T} + \varphi_b + \beta - \frac{\pi}{2}\right) + \gamma_1 m_2 \cdot ab. \tag{10}$$

The working resistance consisted of vertical load, friction force, the self-weight of the top coal, etc.

$$P = G_1 + G_2 + G_3, \tag{11}$$

where $G_1 = V = L_0 q/2$ is the vertical load including the self-weight of unstable THR block D and the overlying soft strata, $G_2 = -T \tan(J_{RC} \lg(KgHJ_{CS}/T) + \varphi + \beta - \pi/2)$ is the friction force exerted by adjacent strata during the instability of the THR, and $G_3 = \gamma_1 m_2 \cdot ab$ is the self-weight of top coal within the roof control distance.

Considering the geological conditions of working face 880 in the Zhuxianzhuang Coal Mine, the following parameters were obtained: $a = 7.147$ m, $b = 1.5$ m, $m_2 = 7.1$ m, $\beta = 65^\circ$, $\varphi_b = 35^\circ$, $J_{RC} = 16.5$, $J_{CS} = 77.79$ MPa, $L_0 = 145.62$ m, $\gamma = 25$ kN/m^3, $\gamma_1 = 13$ kN/m^3, $\gamma_3 = 18.2$ kN/m^3, $H = 60$ m, $H_3 = 65$ m, $q = 2.683$ MPa, $q_0 = 1.183$ MPa, and Kg = 1.0605.

According to equation (10), the factors affecting the working resistance were the fractured block length and thickness, immediate roof thickness, caving coal thickness, basic friction angle, THR fractured angle, etc. The sensitivity curves of the working resistance are illustrated in Figure 7.

According to Figure 7, when the initial fractured block length and thickness increased, the working resistance increased sharply; therefore, they were the sensitive factors during the first weighting. This was because the larger the initial fractured THR size was, the more difficult it was to form a hinged structure with the adjacent strata and the more easily it slid and became unstable. This resulted in the enlargement of the load on the hydraulic support. Therefore, shortening the initial fractured block length and thickness was an effective technical method for the THR precontrol.

3.3. Confined Blasting in Water-Filled Deep Hole Presplit Technology: Weakening Mechanism of the THR. Confined blasting in water-filled deep hole presplit technology (CBWDHPT) took the explosive as energy and confined water (Figure 8) as the blasting medium, making it a highly safe and efficient THR blasting technology [18]. By increasing the wave impedance of the blasting medium in the hole, it could reduce the blasting energy loss [19], strengthen the rock-fracturing orientation of the explosion shock wave, and make most of the "water wedge" cracking and uniform load transfer of confined water [20]. With wedge cutting, the truncated blasting and presplitting weakening of the THR were realized, and the fracturing effect of the surrounding rock was extended, reducing the explosive consumption.

Using the CBWDHPT to weaken the THR made the immediate roof and low-positioned THR in the blasting fracture distribution area fully collapse and fill the goaf timely, supporting the high-positioned THR and preventing its rotation and subsidence. The integrity of the middle-positioned THR in the fracture distribution area was destroyed. The cracks extended along the crack structure under the tensile stress or shear stress, thus changing the boundary support conditions. Cutting off the THR in time and reducing the weighting distance made it possible to control the THR movement.

3.4. Precontrol Technology for the THR. According to the results obtained from the present analysis, it was hard to select hydraulic supports in the case of the natural collapse of the THR. Therefore, the CBWDHPT was proposed to precontrol the THR as follows:

(1) Basic parameters: according to the working face 880 conditions and the expected confined blasting effect, the confined pressure of the water-filled deep hole was 2.0 MPa, the reduction coefficient of the explosive amount was 0.3, and the explosive charge per hole was 32 kg. The horizontal angle of blasting drilling was 15°to 20°, the charge hole distance was 7.0 m, and the diameter of the large pore guidance hole was 100 mm.

(2) Technological process: drilling deep hole ⟶ charging ⟶ hole sealing ⟶ injection of confined water ⟶ blasting ⟶ effect test.

(3) Operation steps: the items associated with this part were briefly presented as follows:

(i) The rock powder in the hole was cleaned with a tamper before charging, and the actual hole depth was determined, recorded, and then charged.

(ii) A special hole sealing device with an injection pipe and drainage pipe was used to seal the hole. The dealing length was generally one-third of the hole depth [21].

(iii) Before blasting, a static pressure water pipe was used to inject water in the charged drilling space after the hole was sealed until the closed drilling space was filled. Water injection in the blasting hole is shown in Figure 9.

(iv) Four shock-wave wind barriers were set, where the roof was complete and the support was intact. Finally, confined blasting inside the roof was carried out after all personnel in the roadway were evacuated.

(4) Computational analysis of the weakening effect of CBWDHPT.

Taking the working face 880 in Zhuxianzhuang Coal Mine as the engineering object, Universal Distinct Element Code (UDEC) software, produced by Itasca (Wuhan) Consulting Co., Ltd., Wuhan City, Hubei Province, China, was used to establish a stope model of the THR. Based on the designed drilling arrangements and parameters, the blasting weakening of the THR was conducted, using the support unit to establish a hydraulic support to analyze the weakening effect [22, 23].

The UDEC model took discontinuous surfaces (joint fractures and cuts) as block boundaries, and joint weakness planes were set in specific rock layers to simulate the weakening effect of the confined blasting. The constitutive relationship between rock blocks and joints in the model was the Mohr–Coulomb plastic model. The specific constraint boundary conditions were as follows:

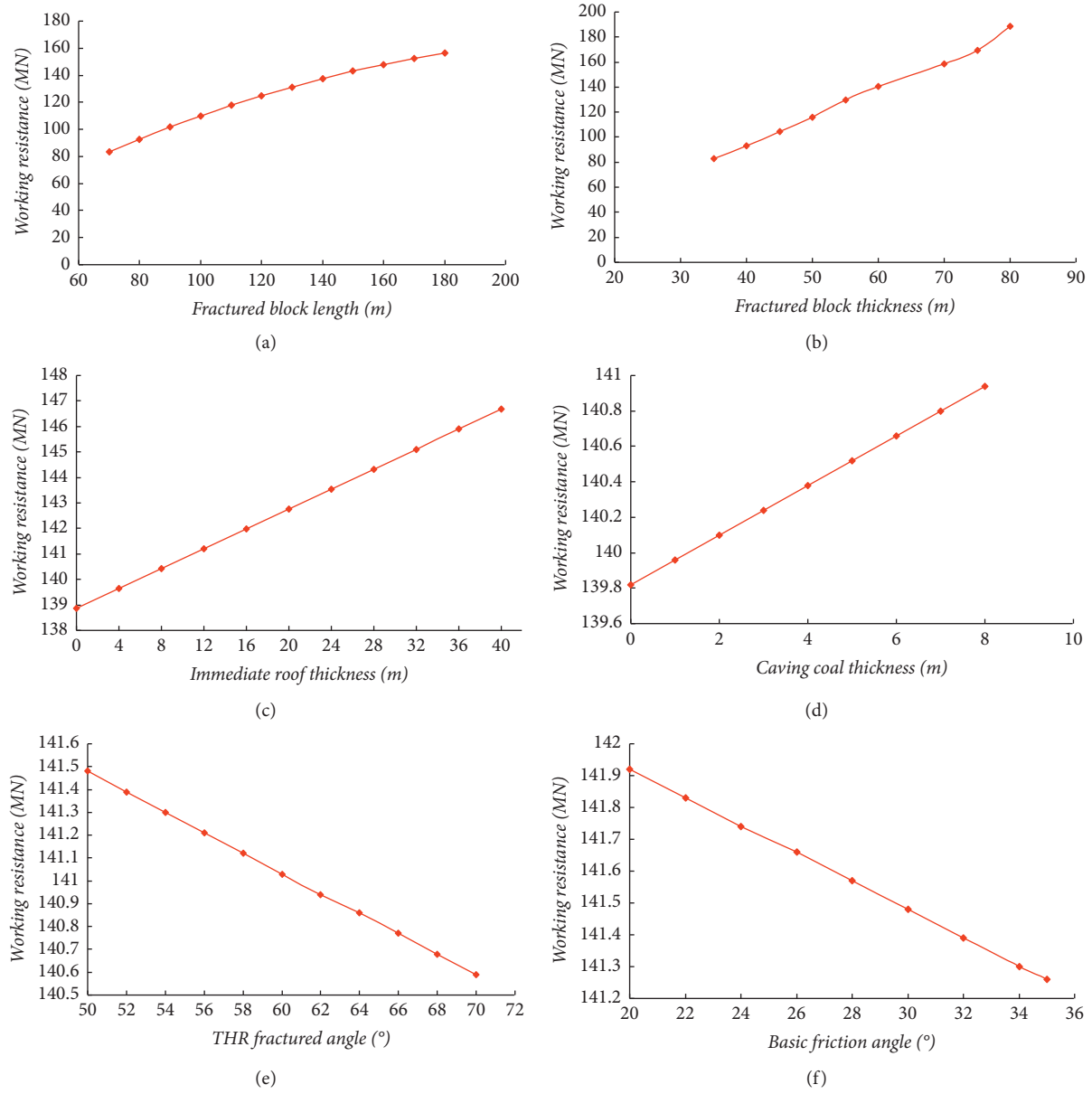

Figure 7: Sensitivity analysis of working resistance during the first weighting.

(i) The displacement vectors and velocity vectors of the left and right surfaces were all 0, the same as the constraint boundary of horizontal displacement

(ii) The bottom surface was a fully constrained boundary—the horizontal and vertical directions were both fixed

(iii) The top surface was a free boundary, and the overlying strata were vertically applied to the top surface boundary in a uniform load

The model was 200 × 160 m (width × height), and the thickness of the coal, the immediate roof, and the THR was 10, 10, and 60 m, respectively. The simulations were carried out in model I without blasting and model II with deep-hole blasting. Layered blasting was conducted on the THR in model II. The upper and lower layers were 40 and 20 m thick, respectively. The lower layer was blasted at an interval of 20 m along the advancing direction.

After the model was established, the coal seam was cut with a distance of 0.85 m/time, and the roof collapse migration and stress distribution evolution under two conditions were obtained, as shown in Figure 10.

Figure 10(a) shows that, as the working face advanced, the immediate roof collapsed periodically, while the THR did not collapse and remained stable with suspension span increasing continuously in model I. The THR blocks, weakened by blasting in model II, collapsed regularly with a certain weighting distance, and the upper THR had better stability under the support of gangue converted by the collapsed THR blocks and immediate roof.

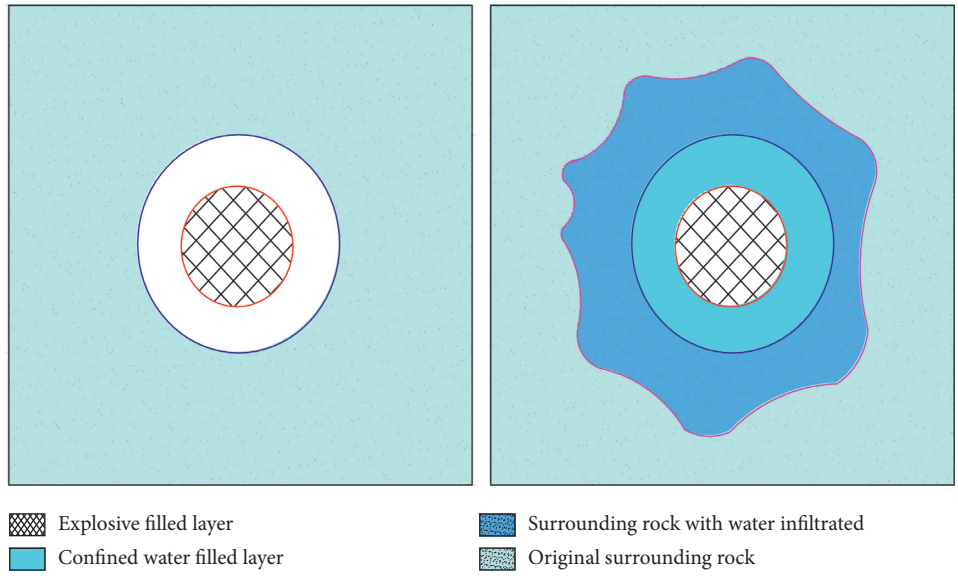

Figure 8: Water-filled confined blasting drilling structure.

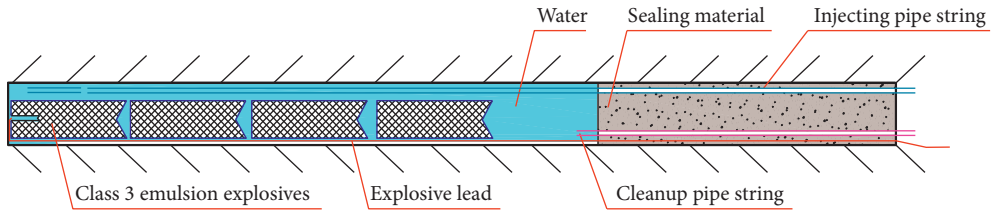

Figure 9: In-hole charge line connecting diagram.

In model I (Figure 10(b)), there was a vertical stress-concentrated area in front of the working face, and the stress peak continued to increase. The maximum vertical stress reached 30 MPa when the working face advanced to 80 m, while it was generally less than 15 MPa in model II.

For working face 880, 87 pieces of ZF13000/21/40 chock-shield hydraulic supports were selected. According to the CBWDHPT parameters in the THR, an industrial test of weakening control was performed in July 2019. The rock fracture and hydraulic support working resistance were monitored on-site, as shown in Figure 11 and Table 2.

Figure 11 shows that the rock collapsed in a large scope due to the blasting weakening effect. The THR broke in sequence to form fragments, blocks, and a strip-shaped rock mass, and the goaf was fully filled. The CBWDHPT charge was only 70% of that in traditional blasting, with the same explosive cartridge and sealing length (26 m). The remaining hole (7 m) was filled with the confined water medium, which achieved good economic benefits.

According to Table 2, the time-weighted average resistance in the working face was 11508.5 kN, accounting for approximately 88.5% of the rated working resistance, and the maximum average value was 12131.6 kN, which was 93.3% of the rated working resistance. This indicated that the hydraulic support had a sufficient safety margin during production. The CBWDHPT of the THR effectively reduced the ground pressure on the working face and achieved a significant application effect.

4. Discussion

3DEC numerical software (3-Dimensional Distinct Element Code, produced by Itasca (Wuhan) Consulting Co., Ltd., Wuhan City, Hubei Province, China) was used to establish the stope model [6, 24]. We defined the ratio of the immediate roof thickness to the coal seam mining height as the immediate roof filling coefficient (N).

According to working face 880, when the mining height was 10 m, the THR thickness was 60 m, and the immediate roof thickness was 10 m, 20 m, and 30 m; the immediate roof filling coefficient N was 1, 2, and 3, respectively. The fracture characteristics of the huge THR are shown in Figure 12.

According to the analysis of the failure characteristics and migration rules of the THR under different immediate roof filling coefficients in Figure 12, it could be seen that when the immediate roof filling coefficients were 1, 2, and 3, the initial and periodic weighting distances of the THR were 140 m and 60 m, 170 m and 70 m, and 210 m and 90 m, respectively. The greater the filling coefficient, the thicker the immediate roof and the larger the goaf filling degree after its collapse. This made the main roof block migration space smaller and the fracture characteristics less obvious. The

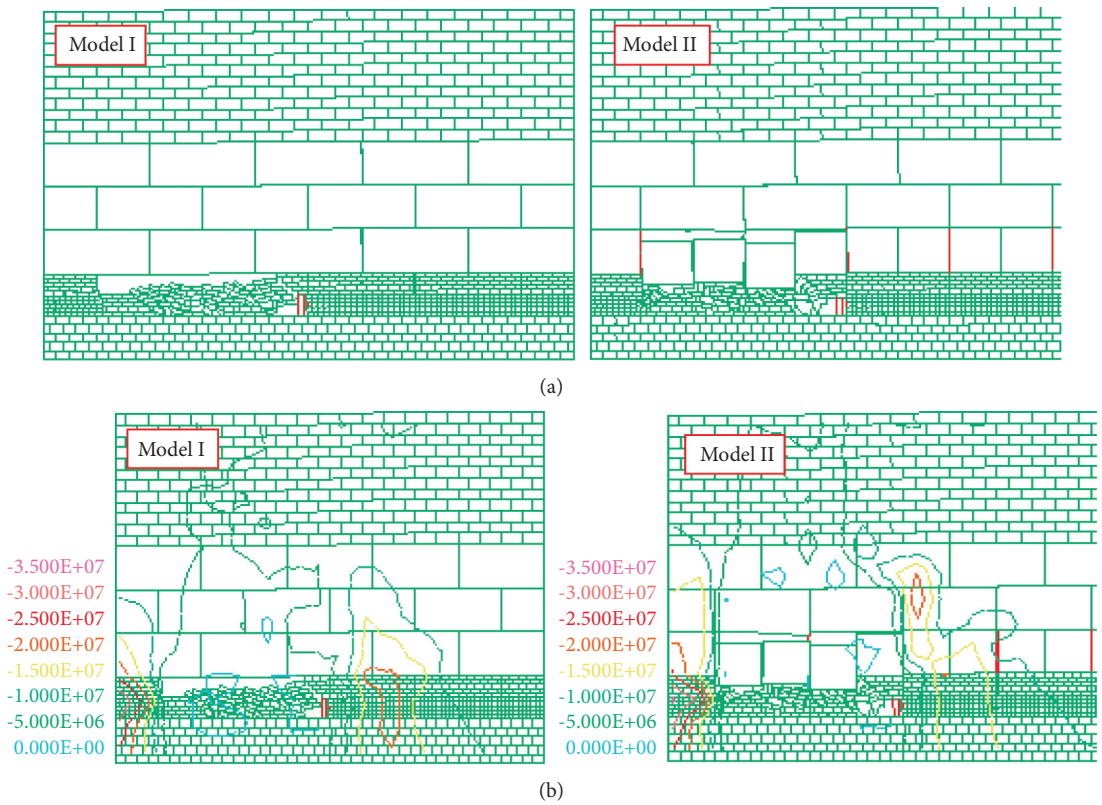

Figure 10: Working face advancing to 80 m. (a) Overlying strata fracture characteristics of the model. (b) Vertical stress characteristics of the model.

Figure 11: Field application effect of CBWDHPT in the working face 880 of Zhuxianzhuang Coal Mine.

Table 2: Characteristics of the working resistance of working face 880.

	Line	Working resistance (kN)		
		Average value	Standard deviation	Maximum value
Maximum resistance	Head position	10111.9	1746.5	11654.1
	Middle position	11955.6	1918.5	12675.4
	End position	11156.3	2442.3	12280.8
	Average	11074.5	2035.7	12203.5
Time-weighted mean resistance	Head position	11008.0	2372.2	11974.7
	Middle position	11864.0	1844.8	12389.5
	End position	11653.8	2353.5	12030.8
	Average	11508.5	2190.2	12131.6

smaller the rock damage height and range, the more alleviated the ground pressure.

We analyzed the displacement distribution characteristics of the overburden strata under different filling coefficients (Figure 13). After the initial failure of the THR with different immediate roof thicknesses, the maximum vertical displacement of the fractured block along the working face strike increased. When $N = 1$, the vertical displacement of the

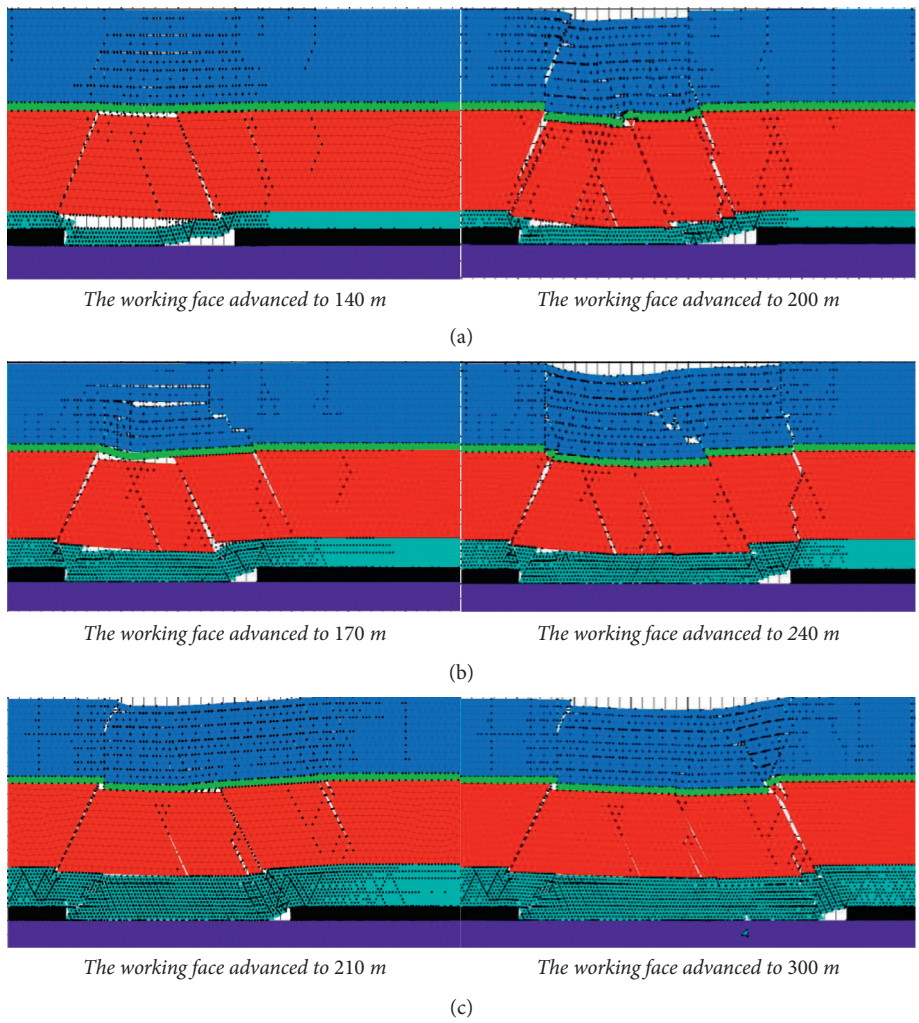

Figure 12: Breakage and migration characteristics of surrounding rocks under different immediate roof filling coefficients. (a) $N = 1$. (b) $N = 2$. (c) $N = 3$.

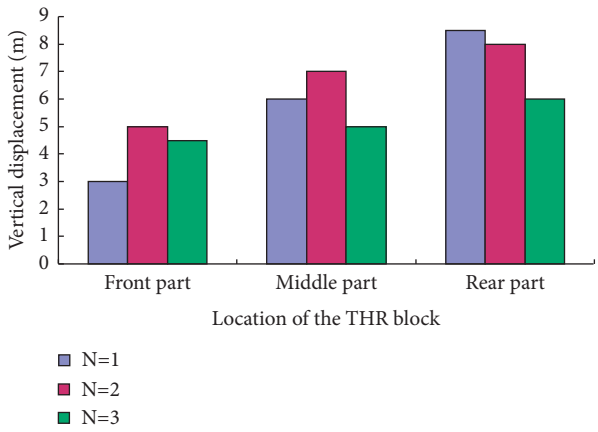

Figure 13: Distribution of vertical displacement of surrounding rocks under different immediate roof filling coefficients.

fractured block changed from 1.5 m to 6 m to 8.5 m; when $N = 2$, the value varied from 5 m to 7 m to 8 m; when $N = 3$, it ranged from 4.5 m to 5 m to 6 m. The changes showed that, after the initial fracture, the block deflected to the working face, and the smaller the immediate roof filling coefficient, the more unequal the fractured block height. The periodical fracture block slipped and lost stability as a whole, and the vertical displacement of the rock block was 7 m, 3 m, and 1 m when the immediate roof filling coefficient $N = 1$, 2, and 3, respectively.

The influence mechanism of the immediate roof filling coefficient was manifested in different restriction degrees on the THR fracture and instability, which affected the fracture position, the fracture size, and the sinking space, thus changing the location and size of the load [25]. The larger the immediate roof filling coefficient, the better the filling degree of the goaf after the immediate roof collapsed and the smaller the sinking space of the THR block.

5. Conclusions

The instability and control mechanism of the THR for safe mining and overlying rock strata protection were studied in this work. Through physical simulation, theoretical analysis, and computational analysis, the fracture characteristics and

instability migration rules of the THR were fully evaluated for determining the precontrol technology and optimizing the hydraulic support type. The main conclusions were as follows:

(1) Large THR breaking span and the sliding instability along the coal wall were the main reasons for support-crushing accidents. Resisting the fracture instability simply by increasing the supporting intensity had limitations, so the effective method for THR control was to reduce the fracture size and movement space.

(2) On the basis of experimental and predicted results, the environmentally friendly strategy for overlying rock strata protection (including the CBWDHPT and support optimization) was discussed.

CBWDHPT was adopted to realize presplitting and weakening control for the immediate roof and low-positioned THR to ensure a timely and complete collapse and filling of the goaf, alleviating the overlying rock strata destruction. The truncation and layered blasting precontrol of the middle-positioned THR shortened the length and thickness of the THR blocks acting on the hydraulic support, reducing the support load and achieving safe mining.

(3) This strategy of overlying rock strata protection was applied in working face 880 of Zhuxianzhuang Coal Mine. In field applications, the THR collapsed and filled the goaf timely, the ground pressure on the working face appeared to be mitigated, and the overlying rock strata evenly subsided. Through the displacement monitoring of overlying rock strata and operation evaluation of the hydraulic support, the effectiveness of the strategy was verified.

Data Availability

The data used to support the findings of this study are available from the corresponding author upon request.

Conflicts of Interest

The authors declare that there are no conflicts of interest.

Acknowledgments

This study was supported by the National Natural Science Foundation of China (52074267), Shanxi Province Science Foundation for Youths Grant (SPSFYG) (no. 201901D211038), Shanxi Province General Natural Fund Project (no. 201901D111049), and Scientific and Technological Innovation Programs of Higher Education Institutions in Shanxi Province (STIPHEI) (no. 2019L0347). This support is greatly appreciated by the authors.

References

[1] B. Sun, P. Zhang, R. Wu, M. Fu, and Y. Ou, "Research on the overburden deformation and migration law in deep and extra-thick coal seam mining," *Journal of Applied Geophysics*, vol. 190, Article ID 104337, 2021.

[2] Y. An, N. Zhang, Y. Zhao, and Z. Xie, "Field and numerical investigation on roof failure and fracture control of thick coal seam roadway," *Engineering Failure Analysis*, vol. 128, Article ID 105594, 2021.

[3] D. Turer, H. A. Nefeslioglu, K. Zorlu, and C. Gokceoglu, "Assessment of geo-environmental problems of the Zonguldak province (NW Turkey)," *Environmental Geology*, vol. 55, Article ID 1001e1014, 2008.

[4] D. Ma, J. Zhang, H. Duan et al., "Reutilization of gangue wastes in underground backfilling mining: overburden aquifer protection," *Chemosphere*, vol. 264, no. 1, Article ID 128400, 2021.

[5] P. Wang, L.-s. Jiang, P.-q. Zheng, G.-p. Qin, and C. Zhang, "Inducing mode analysis of rock burst in fault-affected zone with a hard-thick stratum occurrence," *Environmental Earth Sciences*, vol. 78, no. 15, p. 467, 2019.

[6] T. Zhao, C. Liu, K. Yetilmezsoy, P. Gong, D. Chen, and K. Yi, "Segmental adjustment of hydraulic support setting load in hard and thick coal wall weakening: a study of numerical simulation and field measurement," *Journal of Geophysics and Engineering*, vol. 15, no. 6, pp. 2481–2491, 2018.

[7] L. Jiang, Q. Wu, Q. Wu et al., "Fracture failure analysis of hard and thick key layer and its dynamic response characteristics," *Engineering Failure Analysis*, vol. 98, pp. 118–130, 2019.

[8] Y. Lu, T. Gong, B. Xia, B. Yu, and F. Huang, "Target stratum determination of surface hydraulic fracturing for far-field hard roof control in underground extra-thick coal extraction: a case study," *Rock Mechanics and Rock Engineering*, vol. 52, no. 8, pp. 2725–2740, 2019.

[9] C. Xu, Q. Fu, X. Cui, K. Wang, Y. Zhao, and Y. Cai, "Apparent-depth effects of the dynamic failure of thick hard rock strata on the underlying coal mass during underground mining," *Rock Mechanics and Rock Engineering*, vol. 52, no. 5, pp. 1565–1576, 2019.

[10] F. L. He, S. Gao, G. C. Zhang, and B. Y. Jiang, "Ground response of a gob-side gateroad suffering mining-induced stress in an extra thick coal seam," *Geomechanical Engineering*, vol. 22, pp. 1–9, 2020.

[11] W. Pan, X. Nie, and X. Li, "Effect of premining on hard roof distress behavior: a case study," *Rock Mechanics and Rock Engineering*, vol. 52, no. 6, pp. 1871–1885, 2019.

[12] M. Wang, Z. F. Song, P. F. Gou, and J. Li, "Effect of mining speed on stability control of overburden structure in fully mechanized coal face," *Journal of China University of Mining and Technology*, vol. 49, pp. 463–470, 2020.

[13] T. Liu, B. Lin, W. Yang, T. Liu, W. Xiao, and W. Zha, "Study of effects of hard thick roof on gas migration and field experiment of roof artificially guided pre-splitting for efficient gas control," *Natural Resources Research*, vol. 29, no. 3, pp. 1819–1841, 2020.

[14] M. Ju, D. Wang, J. Shi, J. Li, Q. Yao, and X. Li, "Physical and numerical investigations of bedding adhesion strength on stratified rock roof fracture with longwall coal mining," *Geomechanics and Geophysics for Geo-Energy and Geo-Resources*, vol. 7, no. 1, p. 24, 2021.

[15] W. Huang, X. Wang, Y. Shen, F. Feng, K. Wu, and C. Li, "Application of concrete-filled steel tubular columns in gob-side entry retaining under thick and hard roof stratum: a case study," *Energy Science & Engineering*, vol. 7, no. 6, pp. 2540–2553, 2019.

[16] C. Liu, H. Li, and H. Mitri, "Effect of strata conditions on shield pressure and surface subsidence at a longwall top coal caving working face," *Rock Mechanics and Rock Engineering*, vol. 52, no. 5, pp. 1523–1537, 2019.

[17] Y. Liang, J. Dai, Q. Zou, L. Li, and Y. Luo, "Ignition mechanism of gas in goaf induced by the caving and friction of sandstone roof containing pyrite," *Process Safety and Environmental Protection*, vol. 124, pp. 84–96, 2019.

[18] Q. X. Huang, M. Y. Zhao, Y. L. Tan, and K. J. Huang, "Study of roof double key strata structure and support resistance of shallow coal seams group mining," *Journal of China University of Mining and Technology*, vol. 48, pp. 71–77, 2019.

[19] C. Y. Liu, J. X. Yang, and B. Yu, "Rock-breaking mechanism and experimental analysis of confined blasting of borehole surrounding rock," *International Journal Mining Science Technology*, vol. 27, pp. 795–801, 2017.

[20] J. Jia, X. J. Hao, G. H. Zhao et al., "Evolution analysis of microseismic events before and after mining through large-scale weak zone with high confined water," *Advances in Civil Engineering*, vol. 2021, Article ID 6915221, 12 pages, 2021.

[21] J. Yang, C. Liu, and B. Yu, "Application of confined blasting in water-filled deep holes to control strong rock pressure in hard rock mines," *Energies*, vol. 10, no. 11, p. 1874, 2017.

[22] D. Ma, H. Duan, Q. Zhang et al., "A numerical gas fracturing model of coupled thermal, flowing and mechanical effects," *Computers, Materials & Continua*, vol. 65, no. 3, pp. 2123–2141, 2020.

[23] D. Ma, H. Duan, X. Li, Z. Li, Z. Zhou, and T. Li, "Effects of seepage-induced erosion on nonlinear hydraulic properties of broken red sandstones," *Tunnelling and Underground Space Technology*, vol. 91, Article ID 102993, 2019.

[24] L. Wang, C. He, S. J. Cui, and F. F. Wang, "Numerical simulation of surface movement and deformation caused by underground mining with complex stratigraphic boundary," *Advances in Civil Engineering*, vol. 2021, Article ID 9967071, 14 pages, 2021.

[25] Q. Zhang and D. L. Lopez, "Use of time series analysis to evaluate the impacts of underground mining on the hydraulic properties of groundwater of dysart woods," *Mine Water Environ*, vol. 38, Article ID 566e580, 2019.